Pacific Northwest
NATIONAL LABORATORY

PNNL-33799

Post Access Report

Initial Testing of Wave Energy Powered UV-C LED Anti-Biofouling System

December 2022

Milan Minsky
Linnea E. Weicht
Nichole K. Sather

U.S. DEPARTMENT of ENERGY

Prepared for the U.S. Department of Energy
under Contract DE-AC05-76RL01830

DISCLAIMER

PACIFIC NORTHWEST NATIONAL LABORATORY
operated by
BATTELLE
for the
UNITED STATES DEPARTMENT OF ENERGY
under Contract DE-AC05-76RL01830

Printed in the United States of America

Available to DOE and DOE contractors from
the Office of Scientific and Technical Information,
P.O. Box 62, Oak Ridge, TN 37831-0062
www.osti.gov
ph: (865) 576-8401
fox: (865) 576-5728
email: reports@osti.gov

Available to the public from the National Technical Information Service
5301 Shawnee Rd., Alexandria, VA 22312
ph: (800) 553-NTIS (6847)
or (703) 605-6000
email: info@ntis.gov
Online ordering: http://www.ntis.gov

PNNL-33799

Post Access Report

Initial Testing of Wave Energy Powered UV-C LED Anti-Biofouling System

December 2022

Milan Minsky
Linnea E. Weicht
Nichole K. Sather

Prepared for
the U.S. Department of Energy
under Contract DE-AC05-76RL01830

Pacific Northwest National Laboratory
Richland, Washington 99354

Post-Access Report

Initial testing of wave energy powered UV-C LED anti-biofouling system

Awardee: 3newable LLC

Awardee point of contact: Milan Minsky

Facility: PNNL-Sequim (MCRL)

Facility point of contact: Linnea Weicht

Date: December 16, 2022

Authors: Milan Minsky, Linnea Weicht, Nichole Sather

TEAMER
Testing & Expertise for Marine Energy

1 INTRODUCTION TO THE PROJECT

Biofouling severely limits the quality of data coming from buoy-mounted sensors. Furthermore, incumbent power sources on these buoys have limitations: wind turbines can topple in rough weather and be otherwise damaged, solar panels get contaminated and provide limited power at high latitudes and under cloud cover. While early experience using short wavelength ultraviolet (UV-C) light to prevent biofouling at WHOI has been promising, there are issues with power usage and cost. Co-locating a wave energy converter (WEC) to supply UV-C anti-biofouling units on powered buoy arrays could reduce service frequency by half, from once every 6 months to once every year, enabling major cost savings. Adding efficient power sources for ocean observing sensors will extend operating time, and battery life will no longer be a limiting factor driving maintenance intervals. However, biofouling of sensors and instruments will remain a limiting factor for operation and maintenance of deployed instruments at sea.

3newable is co-developing a unique solution to the biofouling problem together with the Ocean Observatories Initiative (OOI) at WHOI to design and build a buoy-mounted WEC as an integrated power source for a UV-C LED module. The LED module will be designed to retrofit for operation on existing sensors, at optimized wavelength/power/duty-cycle/on-time, and with built-in redundancy.

2 ROLES AND RESPONSIBILITIES OF PROJECT PARTICIPANTS

3newable will be responsible for modification and testing of their existing device under test (DUT) apparatus for use at Marine & Coastal Research Laboratory (MCRL) while MCRL staff will be largely responsible for interfacing wet laboratory resources to the DUT apparatus and carrying out experiments on samples generated.

2.1 APPLICANT RESPONSIBILITIES AND TASKS PERFORMED

1. Engineer the DUT apparatus to accept a PVC input (~3/4”) to provide fresh seawater at a defined water flow rate.
2. Provide all mounting hardware to attached DUT apparatus to mounting beam (McMaster-Carr, Double Six Slot Rail, 47065T109) in horizontal position.
3. Use a PNNL built submersible sleeve for 3newable UV irradiance meter to characterize irradiance at depths to inform test depth of water
4. Provide the DUT apparatus with all electronics (R-Pi microcomputer, camera, lights, led and samples) necessary to monitor testing remotely
5. Work with PNNL to source test coupons to emulate CTD electrodes
6. A 3newable staff will need to visit MCRL for the installation
7. Monitoring the experiment remotely by camera and working with MCRL staff to manage the samples over the course of testing
8. 3newable staff will lead the data analysis and interpretation of results for their report deliverable.

2.2 Network Facility Responsibilities and Tasks Performed

1. Have staff available to consult on engineering above tasks 1, 2, 3, 6
2. Provide mounting beam (McMaster-Carr, Double Six Slot Rail, 47065T109) mounted across 36 inch test tank in horizontal position.
3. Design and build a ¾ inch PVC adapter to supply 3newable with seawater and set up pumping apparatus to supply a controlled flow of fresh seawater
4. Have staff available to support installation of the DUT and monitor the experiment
5. Build a submersible sleeve for a 3newables owned Thorlabs UV irradiance meter
6. Work with 3newables to source test coupons to emulate CTD electrodes
7. Review all design files for safety and compliance with PNNL directives and develop safety/testing documentation to satisfy MCRL standard operating procedures
8. Coordinate with PNNL cybersecurity for permissions to allow 3newable to access a Raspberry Pi that will be hooked up to a camera/assorted peripherals
9. Run tests for weight, conductivity, staining and SEM of samples at given time points
10. Provide 3newable data from testing

3 Project Objectives

The purpose of testing is to determine whether UV exposure of CTD electrode material will inhibit biofouling. The ability of the UV system to temper biofouling growth and combined with a wave energy power source, would provide opportunity for extended deployments of buoyed CTDs at sea. The accumulation of marine growth on deployed equipment is explained by several factors – e.g. location, duration, and seasonality of deployment and associated temperature and light conditions, concentration of biological organisms, material. The test objectives were designed to provide preliminary indication of the efficacy of the 3newable DUT during a six-month period. The three test objectives will provide a combination of quantitative and qualitative data and provide insights into the functionality and effectiveness of the DUT necessary for future optimization and technology readiness levels.

Objective 1. Quantify biomass accumulation on treatment and control electrode materials.

Objective 2. Perform cell staining to measure the prevalence of biofouling on the surface of the electrode coupons.

Objective 3. Collect microscopy imagery of electrode coupons to visualize growth on electrode coupons.

4 Test Facility, Equipment, Software, and Technical Expertise

Facility hardware that will support this testing includes wet labs with 36” water tanks with access to unfiltered seawater pumped fresh from Sequim Bay. Analysis tools include high resolution cameras, precision balances, and biology equipment/reagents required to stain and visualize biofouling. MCRL

staff expertise encompasses the fields of biology, chemistry, and engineering; with specialization in biofouling, electrical and mechanical engineering, microscopy, and applied marine technology.

5 TEST OR ANALYSIS ARTICLE DESCRIPTION– 3NEWABLE

The DUT will embody twin chambers for exposing a sample area with irradiance of 40-80 uW/cm^2 for up to a 10 cm x 10 cm area. This chamber will allow twelve coupons to be exposed in both the UV irradiance area and control sample areas. Surrounding materials serve to channel water over the UV sample and control areas at a defined height and flow rate. The DUT comes with integrated electronics package to allows remote access by 3newable researchers for taking in-situ pictures with an integrated camera and control of lights/UV LED.

The test advances marine wave energy conversion and thermo electric generation system not by increasing power produced, but instead by using generated power to preserve attached equipment for longer duration than currently planned, in essence increasing the utility of whatever device the MRE supports.

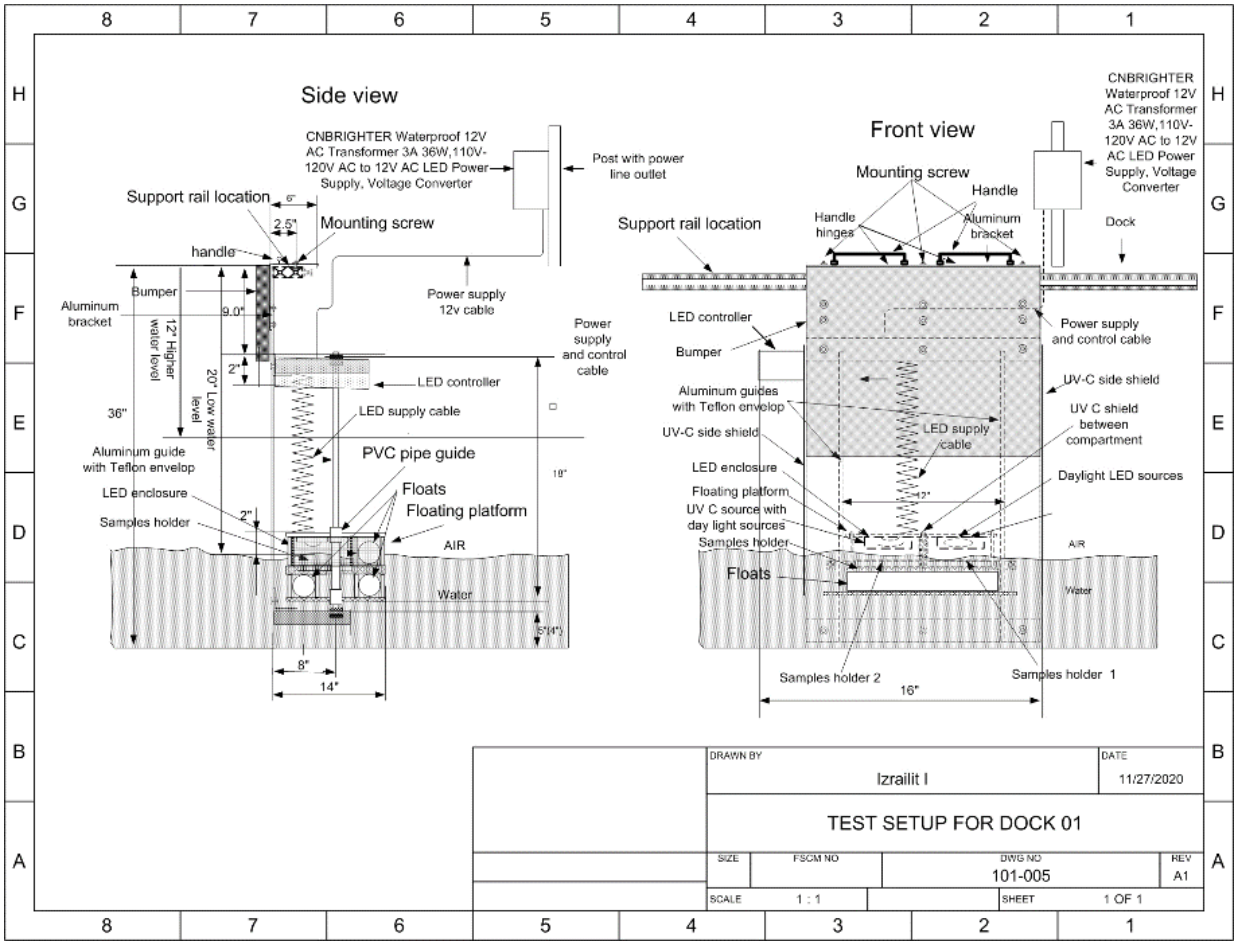

Figure 1. Design of the DUT apparatus. This apparatus will be modified to accept seawater input from a ¾ inch PVC and peristaltic pump input by 3newable and be mounted on t-slot rails in a MCRL test tank.

The following components are necessary to support the test. The relationship among components is visualized in Figure 2.

- PNNL-Devices- The PNNL network connection will provide 3newable remote access to their system
- Raspberry pi- a microcomputer capable of interfacing and controlling peripheral devices
- Camera- A CMOS based camera for visualizing and monitoring the samples remotely
- UV LED- The UV lights source that can be remotely controlled and will illuminate a 10 cm x 10 cm test area
- Light fixture- a light source to allow the camera to take images
- UV Test Area- The area where sample coupons will be placed for testing under UV-C light exposure.
- Control Samples- the area where sample coupons will be placed with identical experimental conditions of the UV light exposed samples. No exposure to UV-C for this sample set.
- Seawater- unfiltered raw seawater will flow over samples under test. Unfiltered seawater contains living micro- and macro- organisms, sediments, and dissolved organic matter that is responsible for bio-fouling.
- Waste treatment- the seawater will be collected and discharged after treatment at the Sequim wastewater treatment facility. No chemical will be released into seawater during this study. All chemical waste will be collected and disposed of as hazardous waste.

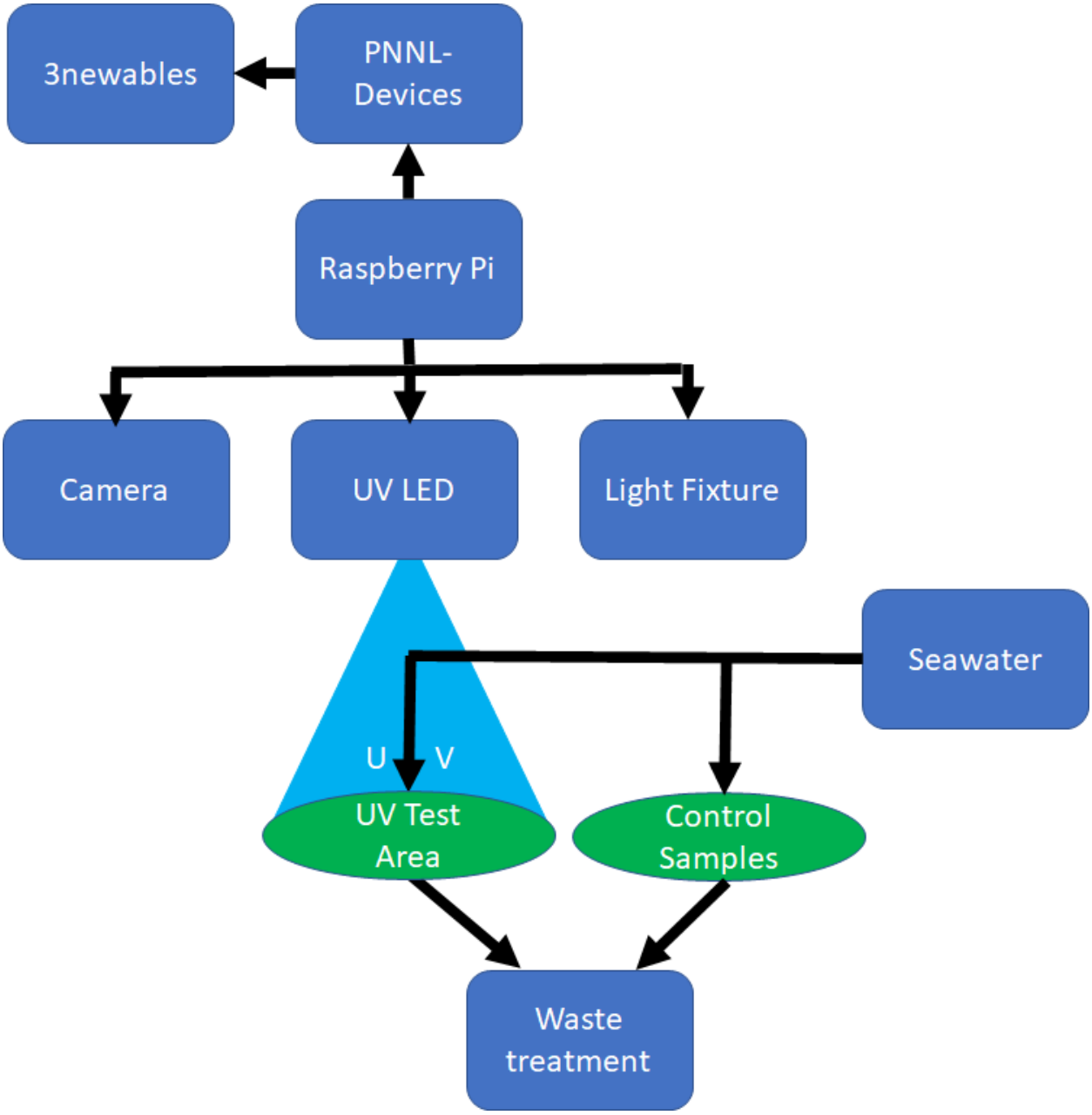

Figure 2. System diagram of the DUT and connections to data and seawater

6 Work Plan

6.1 Experimental setup

Prior to testing a Thorlabs UV meter will be outfitted with a submersible shell and used to determine irradiance at depth and XY offset from UV-C LED. This will give a threshold value for area of irradiance and allow researchers to select water depth for testing. These values will be used by 3newable to

determine the threshold UV radiation reaching the DUT. UV output and depth of penetration through water for DUT will be gathered in mW/cm^2 in 2.5 cm res resolution (XYZ) for 10 cm x 10 cm x 10 cm cube under UV Light water exposure area.

Coupons of electrode material, to emulate the CTD sensors deployed at sea, will be put into a 3x4 grid on the control and UV exposure treatment areas. These coupons will be mounted in the DUT apparatus (Fig 1) that controls seawater flow over the coupons. The apparatus will be mounted in a 36" flow through tank with raw seawater configured to flow over the coupons. Prior to installation in the DUT, all test coupons will be photographed and weighed, and mass recorded for analytical comparison.

6.2 TESTING AND DATA COLLECTION

While testing, a camera installed inside of the DUT will collect daily images of the coupons to document biofouling without physically disturbing the test. The camera will be remotely operated and accessed by 3newables.

To track the efficacy of the anti-biofouling system through time, coupons will be removed from the DUT for testing in groups of three at two-month, four-month and six-month intervals. Coupons will be randomly collected from each treatment, during each sampling interval and analyzed according to the three test objectives.

Biomass accumulation. Wet weights will be collected for the triplicate treatment and control test coupons using a microbalance for growth inhibition comparison. All surfaces but the top (exposed to UV) will be wiped clean with Kim wipes prior to weighing. Weight differences will be quantified in mg difference using a microbalance. Statistical differences determination will be by mean & STD dev.

Cell staining. The cell staining procedure will be applied to coupons using a membrane staining dye. Biomolecular staining of the coupon test surface will be done with a stain trimix containing Erythrosine B, Rhodamine, and Coomassie Brilliant Blue. This staining will enhance the contrast of biological growth on the surface of the test coupon. Qualitative color metric analysis will be calibrated and compared against the control group (no UF-C) to determine non-quantitative growth patterns. A digital library of images will be constructed of both the control and test group.

SEM analysis. Coupons will undergo scanning electron microscopy (SEM) micrograph visualization to determine fate of growth or inhabitation of growth in treatment and control groups. Qualitative results will be used to determine marine life growth inhibition or biofouling surface degradation in the final test group.

6.3 NUMERICAL MODEL DESCRIPTION

N/A

6.4 Test and Analysis Matrix and Schedule

A 4x4x4 matrix of UV radiance values will be generated by either 3newable or MCRL to define the irradiance profile of UV light from the DUT at different offsets relative to the UV LED and depth of the water. Offsets will be +/- 2.5 cm increments up to +/- 5 cm, and 2.5 cm depths. If irradiance values are low as a function of depth then the z-axis will be adjusted accordingly to generate meaningful data.

Tests for the following factors will be taken and compared between the UV treatment and control groups at two, four-, and six-month timepoints.

Table 1: Test Factors

Test	Units
Weight	grams
Membrane stain	Intensity (vs calibrated color bar)

6.5 Safety

All work scopes and funding must be authorized by one or more responsible managers, depending on the type of work being performed, and all work activities conducted in laboratory or operations spaces must be conducted under a project management office director approved electronic prep and risk (EPR) and appropriate work planning and controls.

Hazards and risks associated with the work follow the requirements in hazard-specific work controls and are reviewed with assistance from the PNNL Safety and Health representative, and/or a PNNL subject matter expert (SME).

Plan controls to mitigate hazards in the following order:

1. ELIMINATION OR SUBSTITUTION OF HAZARDS
2. ENGINEERED CONTROLS
3. WORK PRACTICES AND ADMINISTRATIVE CONTROLS
4. PERSONAL PROTECTIVE EQUIPMENT.

Determination of appropriate work controls relevant to the work performed are found in a PNNL Lab Assist document. A Lab Assist activity is a central document that includes work controls, applicable

training, associated hazards, approved lab spaces that all workers must review and acknowledge before performing work. For activities outside of laboratories, work will follow the risk mitigation approach documented in the project management plan or off-site risk management plan for the project.

6.6 Contingency Plans

The Sequim PNNL facility has backup generators that power the entire facility in the event power is interrupted from the public utility district. These generators are configured to start up automatically in the event of a power interruption.

Where possible, back-up equipment and DUT parts (e.g., water pumps, hoses, etc.) will be keep onsite for immediate replacement in the event of failure. Daily monitoring via remote access camera, by 3newable, will help to rapidly intercede in the event of unforeseen equipment failure.

6.7 Data Management, Processing, and Analysis

6.7.1 Data Management

Streamed data, via the camera installed with the DUT will be managed by 3newable. Laboratory generated data (biomass, conductance, imagery) will be stored internally on PNNL servers, backed up through an access-controlled cloud-based shared drive (MS Sharepoint and/or OneDrive) and provided to 3newables for analyses, evaluation, and reporting.

6.7.2 Data Processing

6.7.3 Biological growth data for weight and staining efficacy will be processed in triplicate and allow for statistical analysis for mean and standard deviation of mass and intensity to test for significance. PNNL staff will complete statistical analyses and help 3newable interpret test results.

7 Project Outcomes

7.1 Biofouling Results

7.1.1 Coupon Nomenclature

Twenty-eight coupons were provided for this experiment, resulting in four sets of triplicates for each control and treatment sets, as well as four coupons allocated for initial process testing. Coupons were formed of 1 inch by 1 inch by 1/8 inch platinum-coated titanium and weighed approximately 9.4 grams each.

Coupons were assigned identifiers based on location in 3D printed coupon trays to assist in data organization. As depicted in Figure 3, the tray's rows are lettered A through D, and the tray's columns are numbered 1 to 4. Additionally, a '-T' is added to coupons in the treated sample set, and a '-C' is

added to coupons in the control sample set. Trays were also printed in different colors (blue for treated and black for control) to assist in keeping control and treated coupons separate.

Figure 3. Coupon identifiers based on tray location

7.1.2 Biomass Data

Biomass data were collected for each coupon before the experimental campaign began. Wet weights were collected for triplicate treated and control test coupons using a microbalance to compare growth inhibition. Biomass data was calculated as initial coupon mass subtracted from the final wet mass for each biofouled coupon. Compiled mass-gain per coupon is organized in an Excel document 'Triplicate_Weights.xlsx.'

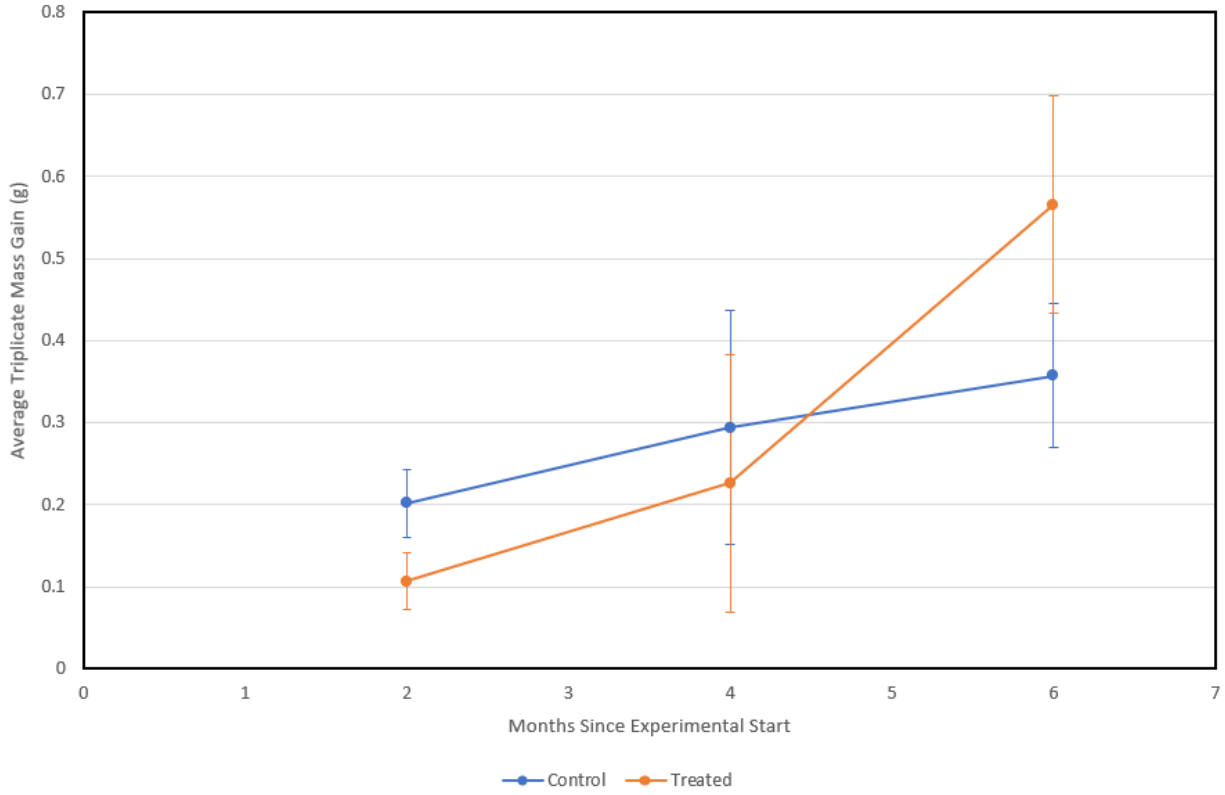

Figure 4. Average triplicate set weight-gain at three time points over six months with error bars representing standard deviation of the respective triplicate sets

While initial biomass data (month 2) demonstrated an increase in biofouling on control test coupons relative to treatment coupons, average mass of treated coupons was higher than control coupons in the final datapoint. Both sets of coupons, as seen in Figure 4, ultimately revealed increasing biofouling throughout the course of the experiment.

The biomass of biofouling was compared using a general linear model. Main effects included the treatment type (control or UV treatment) and duration of the experiment (2, 4, or 6 months). The interaction of type and time were also included in the model. Pairwise comparisons of mean biomass were examined using the Tukey method with a family error rate of α of 0.05.

There was marginally significant interaction between treatment type and duration (GLM: $F_{(2, 17)} = 3.49$, $p = 0.064$). This indicates that biomass of fouling on the coupons depended on the treatment type and time samples were collected (Figure 5). Given the significant interaction term, pairwise comparisons of the term were used to evaluate whether there were statistically significant differences between the treatment and control groups within a given time period. For example, a comparison of treatment coupons during month two vs. control coupons during month two. During the three time periods – month two, month four, and month six – there were not significant differences between treatment and control groups ((Tukey post-hoc $p = 0.888$, $p = 0.970$, and $p = 0.259$, respectively).

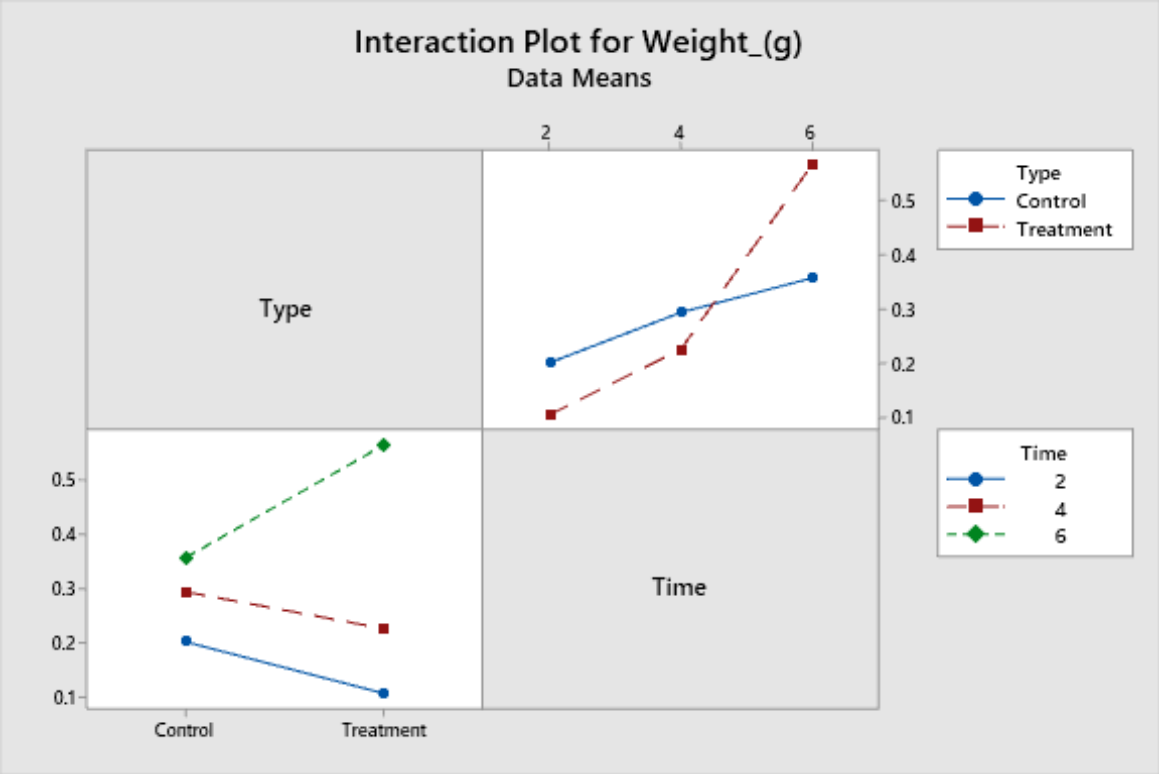

Figure 5. Interaction plot for mean coupon weight (g) for each treatment and time (month)

7.1.3 Image Data

After collecting biomass data, coupons were photographed in triplicate in order to provide another quantifiable metric to track biofouling growth. After initial photographing, coupons were stained using a tri-mix dye containing Erythrosine B, Rhodamine, and Coomassie Brilliant Blue, causing biofouling to pick up red, blue, and purple hues. This dye was allowed to sit on the coupons for one minute and they were photographed again. The coupons were then rinsed in filtered seawater to remove excess dye and photographed a third time. The stain enhances contrast of biological growth on the surface of a coupon as compared to the coupon itself, which can be processed through a software to determine the percentage of gray, red, green, and blue hues found on a coupon, quantitatively indicating amount of biofouling buildup.

Resulting photographs of stained coupons after rinsing with filtered seawater was processed by PNNL's BGI (Biofouling Growth Indicator) software. Results include quantitative percentages indicating the area and intensity of biofouling coverage as picked up by the software in color-scales of gray, red, green, and blue (Larimer et al).

7.1.4 Image Results

Month 2: 5/19/2022

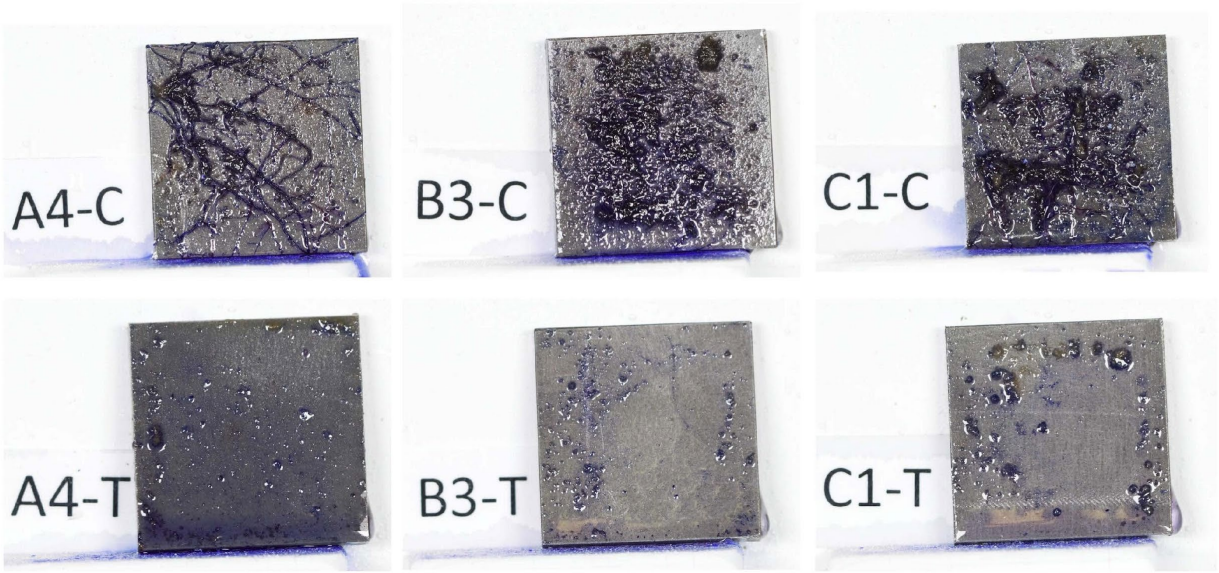

Figure 6. Biofouled coupons selected for analysis at the two-month datapoint, after staining and rinsing for image analysis

Month 4: 7/21/2022

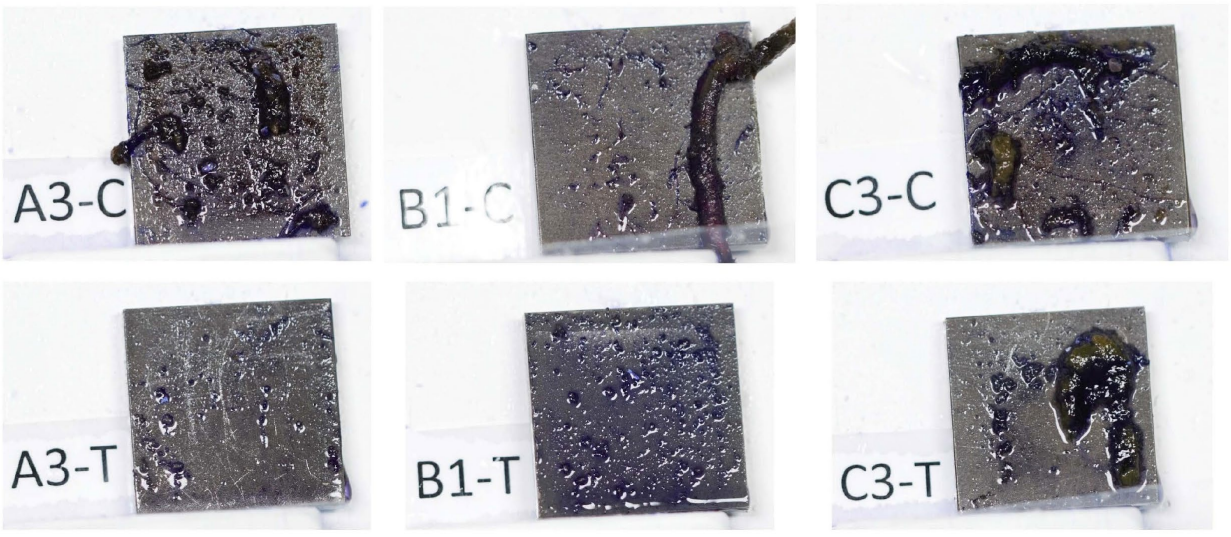

Figure 7. Biofouled coupons selected for analysis at the four-month datapoint, after staining and rinsing for image analysis

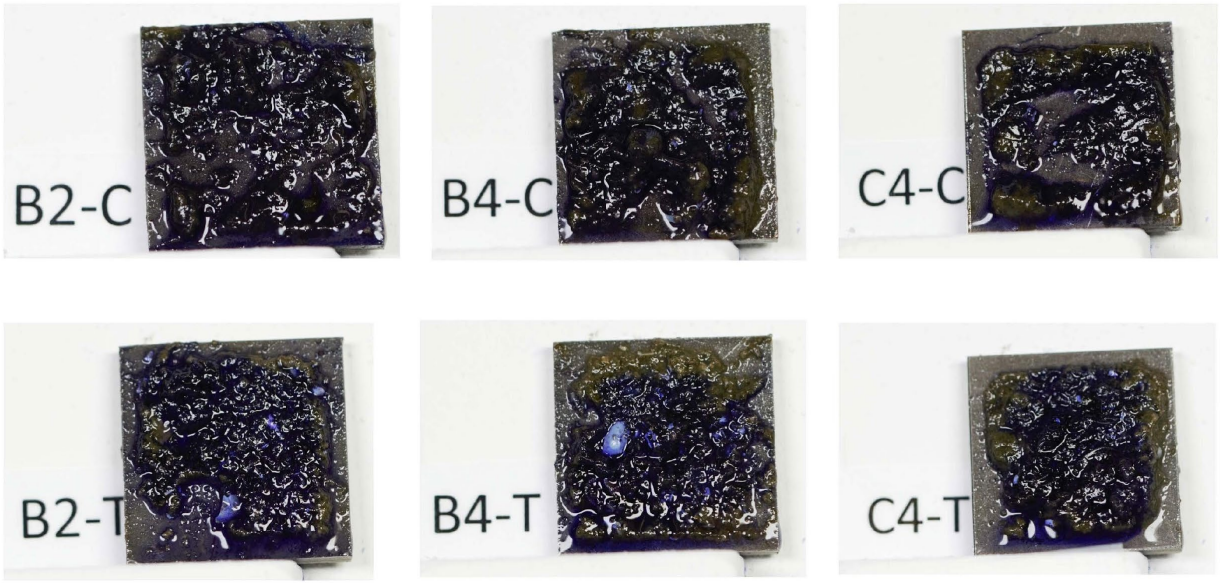

Figure 8. Biofouled coupons selected for analysis at the six-month datapoint, after staining and rinsing for image analysis

Images of the final stained and rinsed biofouled coupons for analysis at each datapoint are included in Figure 6, Figure 7, and Figure 8. Images were analyzed using a control patch of stained coupon without biofouling selected from a clear area of each coupon respectively. The individual controls, rather than using a single control coupon to compare stained biofouling with, avoids skewing data due to slight variation in coupon hues. This phenomenon can be seen when comparing control and treated A4 coupons – the treated coupon has a darker base coloring, which should not be identified as biofouling.

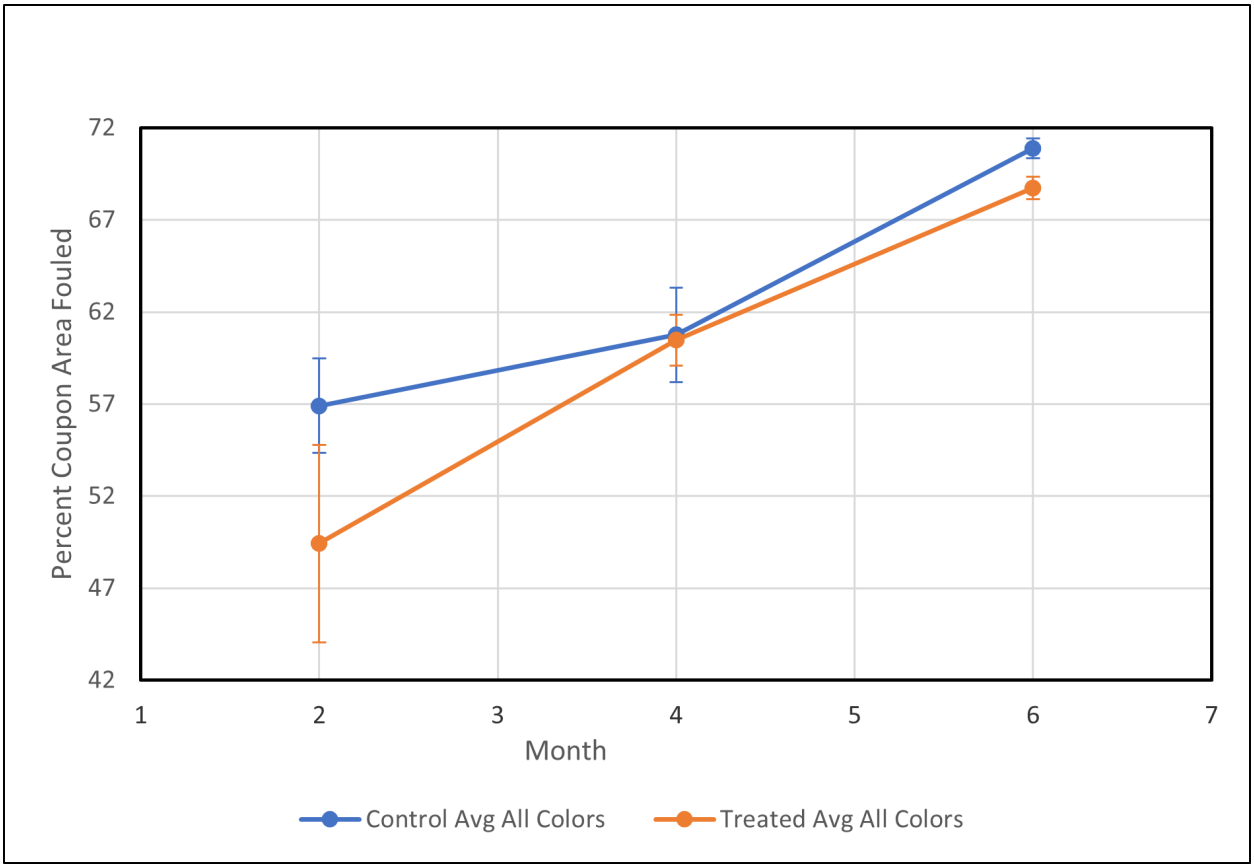

Figure 9. Average of gray-, red-, green-, and blue-scale percentage biofouled results produced by PNNL's BGI software. Error bars indicate standard deviation.

BGI software results indicate similar biofouling growth on control and treated coupons for each of the three time points. The fourth month sampling, July, produced very similar percent area biofouled results for both treated and control coupons. However, during this data collection several worms were found in the control coupon tray, one of which can be seen growing on coupon B1-C. A dramatic increase of biomass in month 6 results is visually observable, as notable areas of each coupon were covered in algae.

The percent cover of biofouling on test coupons were analyzed using PERMANOVA+ for PRIMER-e (Anderson et al. 2008). This analysis assessed differences in percent cover according to intensity of color from images of stained coupons and included factors of treatment type (control or UV treatment) and duration of the experiment (2, 4, or 6 months). Data were square root transformed and a Euclidian distance-based resemblance matrix was calculated. An ordination plot using non-metric multidimensional scaling was used to visualize the similarities among samples according to the two factors, treatment type and month. Model-based analyses were performed using permutational multivariate analysis of variance (PERMANOVA) to test for statistical differences among factors including treatment type and duration of the experiment.

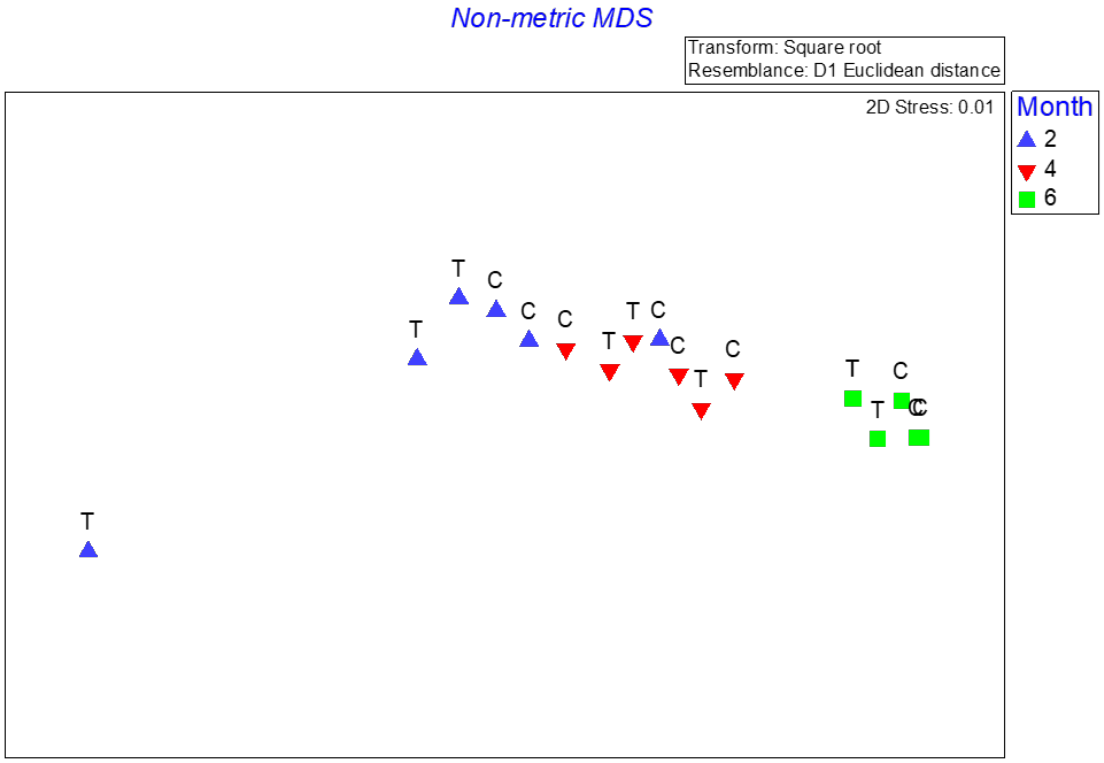

Figure 10. Non-metric multidimensional scaling plot of percent cover of biofouled surface on coupons. Letters on the plot correspond to "control" or "treatment" samples. Symbols correspond to the month when samples were analyzed.

The non-metric multidimensional scaling (nMDS) plot indicates similarities in percent cover of the biofouled coupon surfaces between treatment and control groups within a given time period (Figure 10). Bootstrapping is another visualization technique that provides an estimate of the means, via resampling, for each of the factors along with regional estimates around each mean (Figure 11). The MDS bootstrap averages show some overlap between the treatment and control groups with greater variation in averages associated with the treatment group. The MDS bootstrap averages were distinct for the three time periods with greatest variation during month two (Figure 11).

Treatment type explained six percent of the variation in the modeled data and was significantly different (Pseudo-F = 0.293, p = 0.0525). Months explained 70% of the variation in the data and was significantly different (Pseudo-F = 25.4, p = 0.0001), and the interaction between sample type and month was not significant (Pseudo-F = 2.16, p = 0.125). Thus, according to the multivariate analysis, treatment of the coupons does have an effect on biofouling growth; however, that effect is considerably less than the effect of time on biofouling growth.

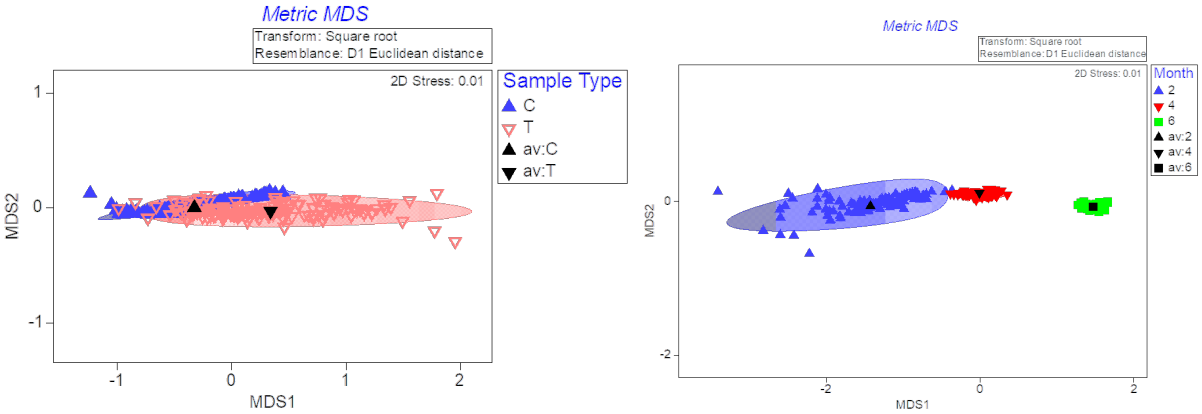

Figure 11. Metric multidimensional scaling using bootstrap averages of percent cover of biofouled surface on coupons for treatment and control groups. Solid black symbols are the group averages. Shaded areas are the 95% confidence regions of the bootstrapped values.

Several of the BGI results are not intuitive. For example, month 4 BGI analysis produced nearly identical average treatment and control coverage results, while visually inspecting the coupons indicates a higher coverage on the control coupons. The BGI biofouling software was designed to quantify small amounts of biofouling, where it is difficult to determine visually which coupons are more fouled. This should be considered when analyzing results, as the amount of fouling on most coupons in both the treatment and control groups was greater than that intended for the software's use. Additionally, glare that reflected off water droplets created a light upper end of the color spectrum in each image. That range may also contribute to skewed BGI results.

To address some of these confusing factors, each image was converted to grayscale and pixels with low brightness identifiers (dark gray and black pixels) were considered biofouled. Using Matlab, the percentage of pixels considered biofouled was calculated for each image, and the results are presented in Figure 12.

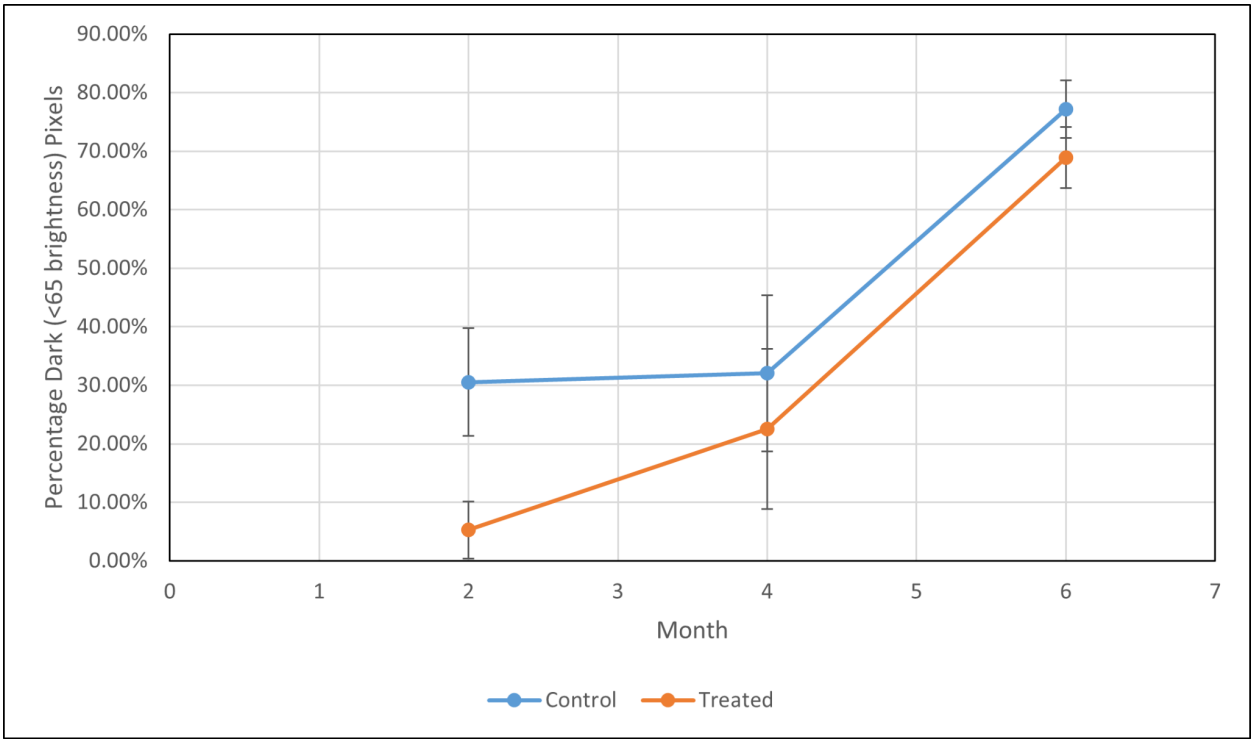

Figure 12. Biofouling calculated as percentage of dark pixels in grayscale image by month for control and treated coupons

These results more closely resemble the visual appearance of biofouling, where control coupons from month 4 do not appear much more biofouled than control coupons from month 2; however, treated coupons gradually increase in biofouling over that period. The considerable leap in biofouling from month 4 to month 6 for both sets of coupons is also more clearly visible in the pixel analysis than in the BGI results.

7.1.5 Scanning Electron Microscopy (SEM)

Three coupons from each treated and control set were randomly selected for scanning electron microscopy in month 6. The coupons selected are depicted prior to analysis in Figure 13. Samples were dehydrated using an ascending ethanol series and imaged with a focus on unique or remarkable organisms. A sample of the resulting SEM images is displayed in Figure 14.

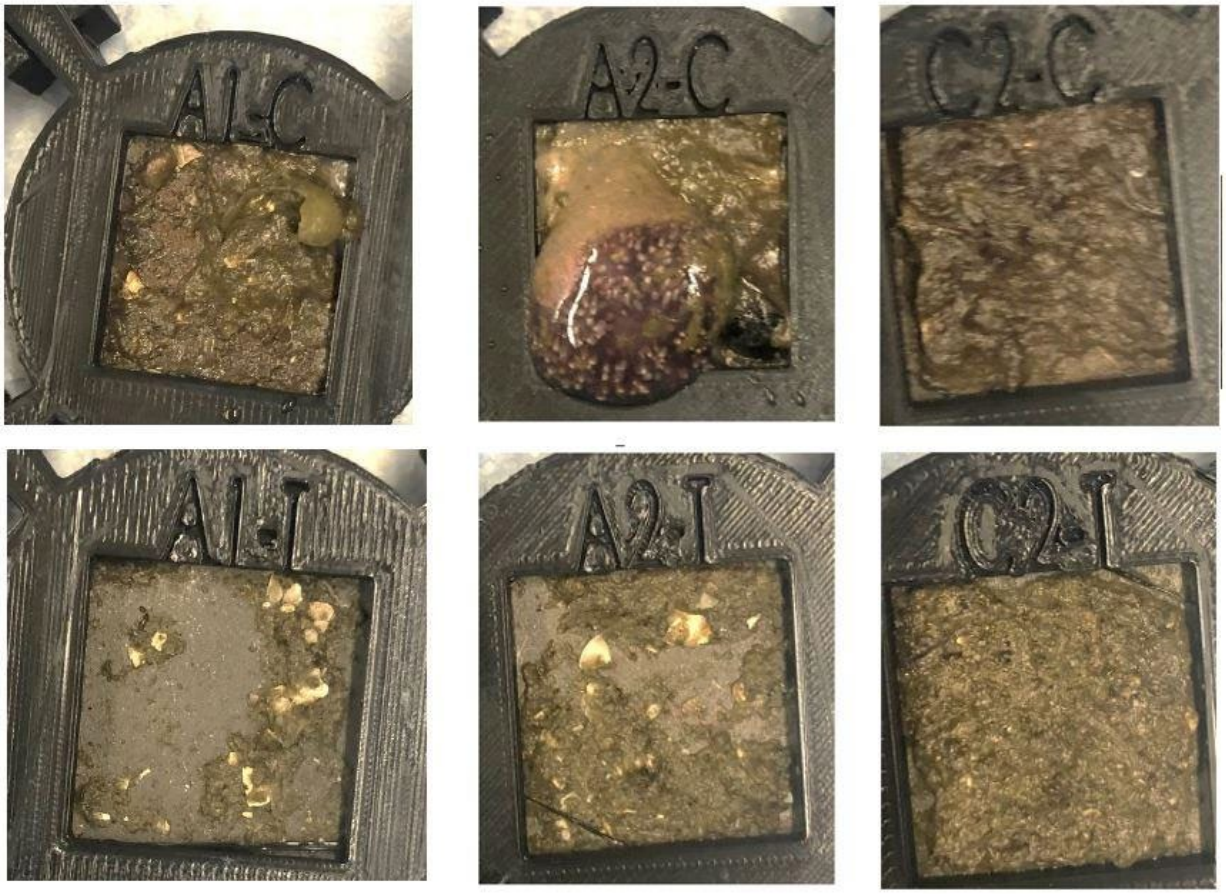

Figure 13. Control [C] and treated [T] samples selected for scanning electron microscopy analysis prior to dehydration

SEM imaging resulted in the discovery of diatoms on each of the coupons. This was unsurprising, as a visible algal layer covered the surface of each coupon, seen in Figure 13. Several coupons contained more advanced lifeforms, such as small shrimp, crustaceans, and mollusks. Shell particulates were found on both control and test coupons, which was likely caused by shells moving through the water column and becoming entrapped in the algal biofouling on each coupon. The crustaceans were found on both control and treated coupons, which again may have been living on the coupons, or may have become entangled in the algae after moving through the water column. Larger mollusks appeared on two of the control coupons, and most notably a large invertebrate, likely a stalked colonial tunicate appeared on control coupon A2-C. The larger organisms such as large shells and the tunicate only appeared on control coupons.

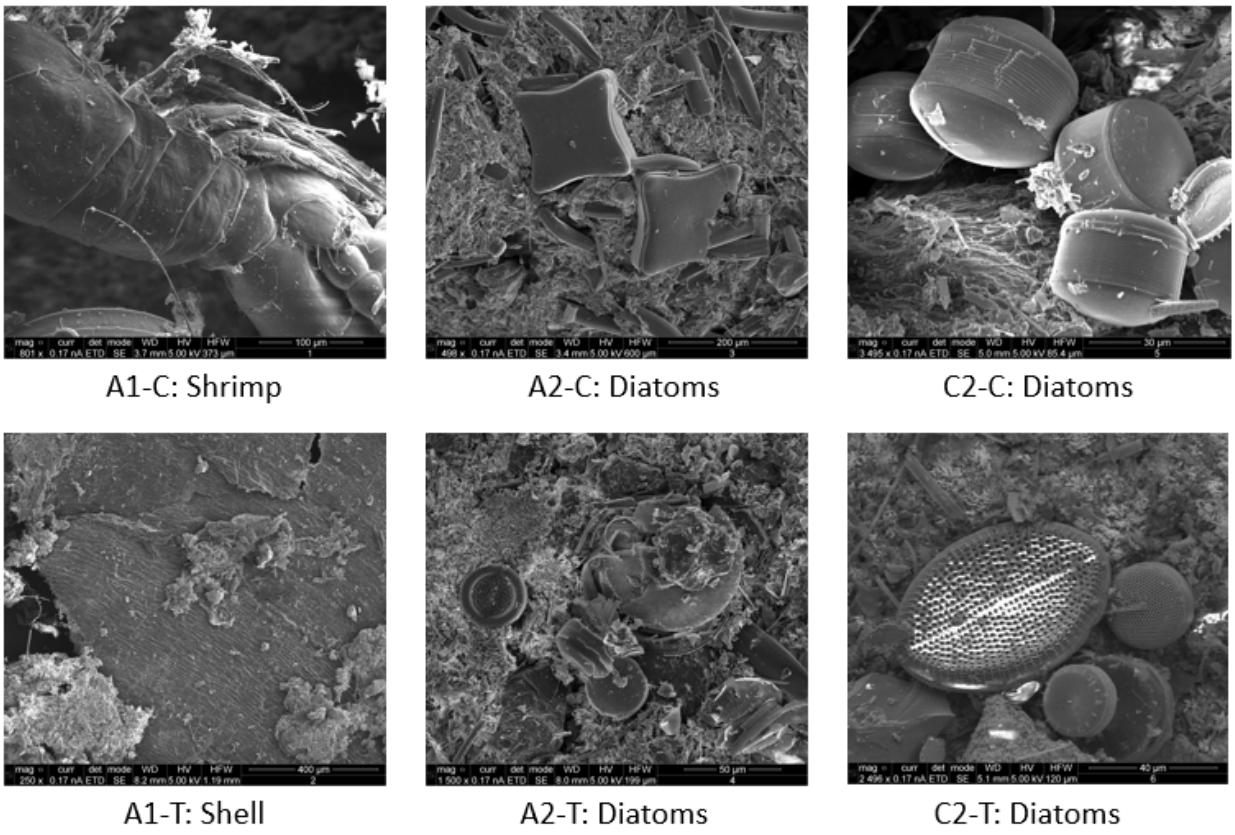

Figure 14. Singular SEM images from each control [C] and treated [T] coupon selected for analysis.

Coupons were also photographed in profile to assist in characterizing thickness of material buildup. Dry weights of the biomass were collected after SEM analysis to assist in characterizing material buildup quantitatively. Results are listed in Table 2.

Table 2: SEM coupon material dry weights

Coupon ID	Weight Control (-C) [g]	Weight Treatment (-T) [g]
A1	0.519	0.434
A2	0.613	0.548
C2	0.553	0.598
Mean	0.562	0.527
Standard Deviation	0.0476	0.0841

Control coupons averaged a higher weight of biomass compared with treatment coupons selected for SEM analysis. This aligns with a visual inspection of the coupons in profile (Figure 15), as control coupons appeared to carry thicker material buildup than corresponding treatment coupons.

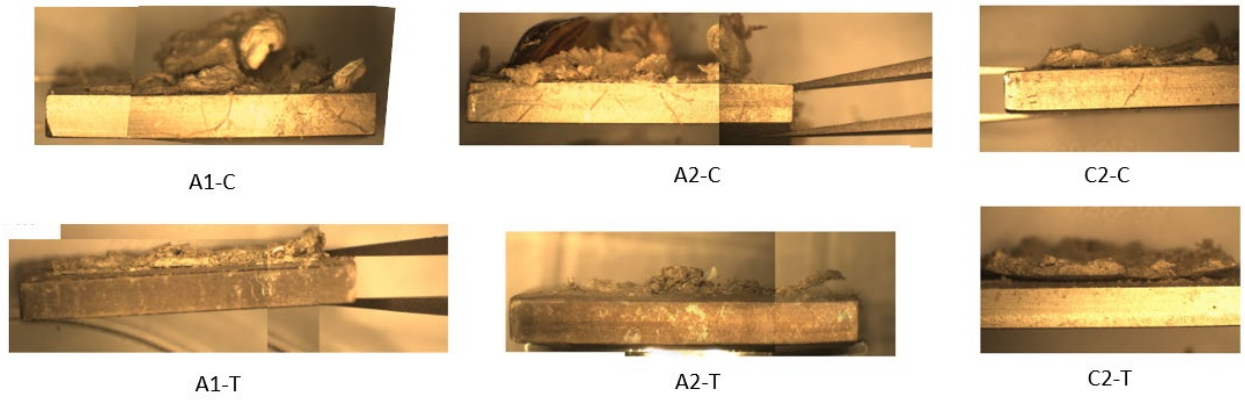

Figure 15. Profile views of coupons after dehydration for SEM analysis

7.1.6 Images from Camera in Test System

Images in Figures 16 and 17 shown below were taken approximately 3.5 months after the beginning of the experiment. These camera images support the quantitative (Figure 12, lower percentage of coverage on treated than untreated coupons) and qualitative (Figure 15, profile SEM views with more material accumulated on control as compared to the treated coupons analyzed) results presented above, showing that in months two and four, before the algae bloom, test coupons analyzed from the chamber outfitted with UV-C light had less material/growth than the control chamber.

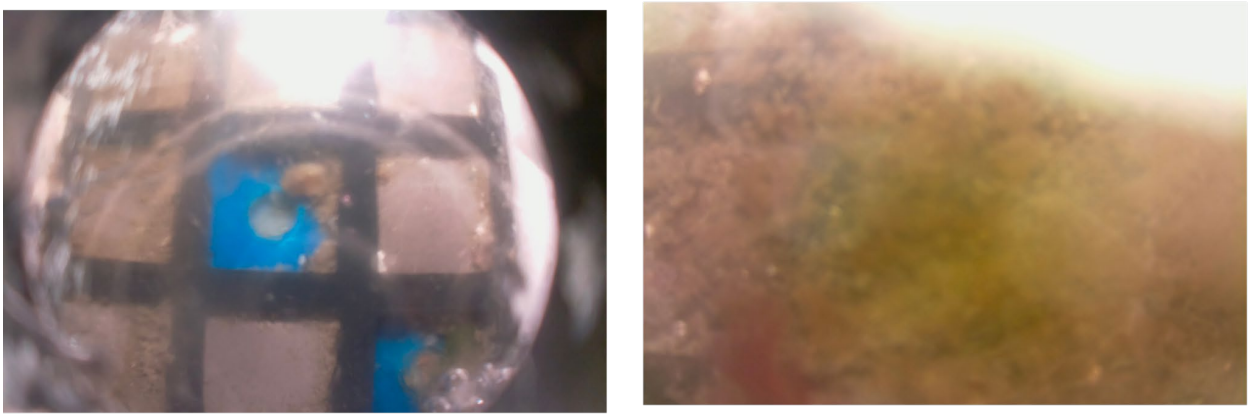

Figure 16. Images taken by the system camera (left) Chamber treated with UV-C (right) Control chamber, both shown on July 12, 2022, about 3.5 months after start of testing

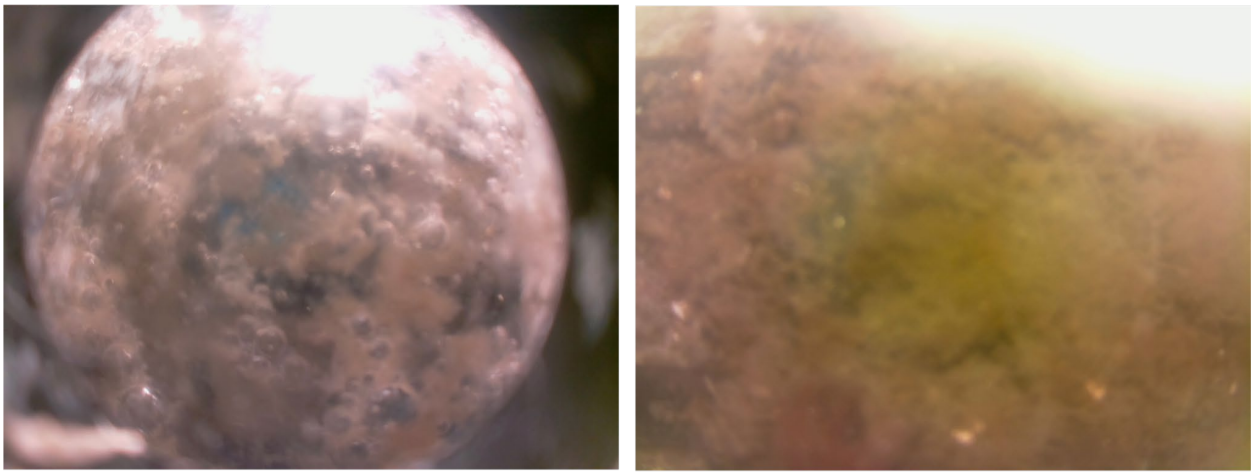

Figure 17. Images taken by the system camera (left) in chamber treated with UV-C and (right) control chamber, both shown on July 17, 2022, about 3.5 months after start of testing, images may be showing impact of an algae bloom

7.2 Water Temperature

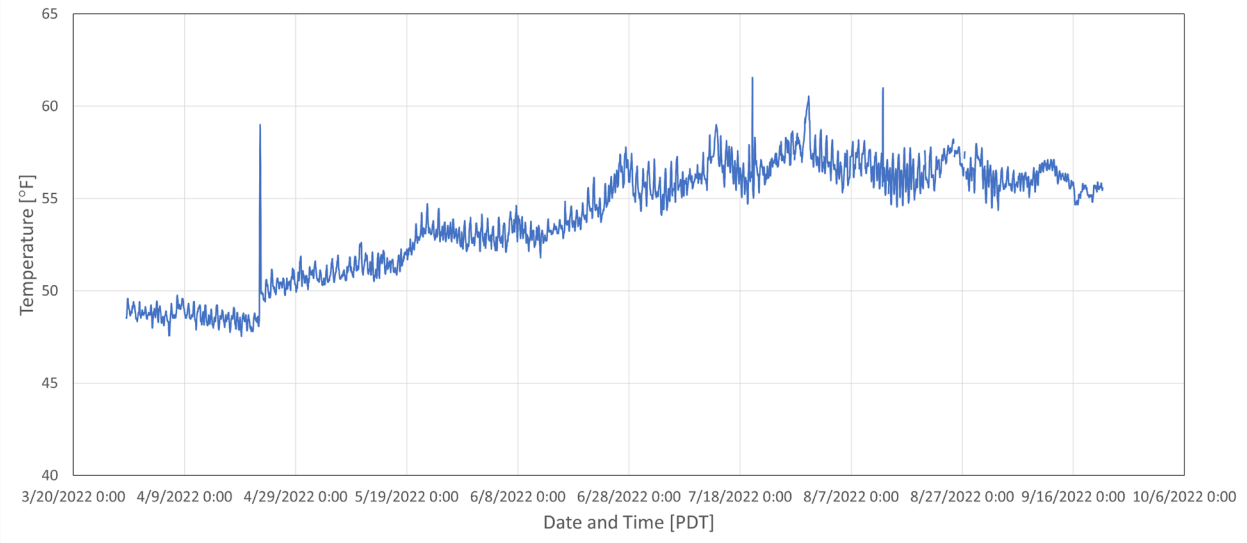

Figure 18. Tank water temperature over the duration of the experiment. Unreasonable spikes in temperature between 100°F and 200°F have been removed, and the data has been smoothed using a moving average across two hours.

Tank water temperature varied slightly from the start of the experiment in late spring, when temperatures were between 45°F and 50°F, and the end of the experiment in full summer when they reach above 60°F.

7.3 UV-C Irradiance

Figure 19 shows a simple map of microwatts/cm^2 measured by the Thorlabs power meter and an overlay showing approximate coupon locations. There are a few things to note here. Because of the size of the power meter head, we were not able to measure the irradiance level corresponding to the exact location of each coupon location individually, but the distribution is representative. In general, there is

not a strong dependence on microwatts/cm^2 observed for the cleanliness of a specific coupon on power level. This suggests that any statistically significant impact of the UV-C light on biofouling inhibition was present at even the lower power levels used here, which is encouraging. Based on these results, we anticipate that with recent improvements in LED power from our supplier we will be able to achieve at least the level of inhibition demonstrated here or better, for our planned open ocean testing with the CTD sensor.

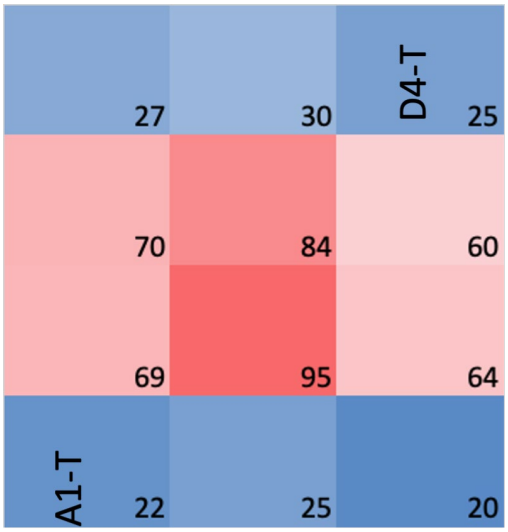

Figure 19. Irradiance level (microwatts per centimeter squared) distribution measured by Thor Labs UV-C power meter at sample/coupon tray

7.4 Discussion

The coupons in both treatment groups, as seen in Figure 8, revealed increased biofouling by weight between months 4 and 6. This timeframe began July 21st and ended September 20th, during which time temperature peaked at approximately 60°F. The increase in temperature may have contributed to the increase in biofouling growth on both sets of coupons.

There were some statistical differences between the treatment groups; however, there were also some notable similarities in biofouling characteristics. This may be due to one or more possibilities. After the experiment ended and the test rig was extracted from the tank, biofilm was noted on the camera enclosure glass. This biofilm was minimal; however, it indicates the presence of water and/or biofouling reaching the camera enclosures and potentially blocking UV-C irradiation or increasing depth of water for light to attenuate through. This, or an algae bloom that occurred at the end of July, may have limited the efficacy of the UV-C treatment in the last few months. Additionally, the test enclosures contained numerous approximately ¼" holes to allow water drainage, but any algae larger than the holes in the test chambers would remain trapped in the chambers and potentially block UV-C rays from reaching the test coupons. The factors potentially reducing treatment efficacy may be an artifact of the experimental setup (confined chambers trapping biofouling, distance UV-C irradiation must attenuate through), but

they provide valuable insight into the risks that must be considered for an at-sea deployment. Any future design would ideally reduce confined spaces and locate the treatment source close to the target receptor.

This experiment was conducted with a water depth of approximately a little less than half the test chamber height (1.35") and the impact of attenuation by water on UV-C efficacy needs to be accounted for. We had originally intended to measure UV-C light attenuation as a function of water depth in the test chambers, using a specially designed 3-D printed sheath together with a UV-C detector made by Thorlabs (PM 120VA for UV-C light detection). However in the end the concern about damaging the (expensive) Thor Labs detector and the availability of data on attenuation in sea-water led us to do the measurements in air at the coupon tray location to map variation in uW/cm^2

We used data from Armstrong et al on the ultra-violet absorption of sea water to estimate absorption effects. From this data attenuation of the 275 nm light by 1.35" of sea water was limited, and an estimated 93% of the UV-C light reaches the treated area.

Light output from the "solar" (warm white) LEDs was not measured, but the same design was used for both chambers and therefore illumination from these LEDs, to promote biofouling, was assumed to be the same.

Despite the increase in algal biofouling over months 4-6, there was a difference in the life forms observed in each test chamber. The control chamber (solar only) produced at least three worms, two of which were tube worms (one observed at month 4 sample collection and another at month 6) and one of which was a 15-scaled worm (observed at month 4). On the samples selected for SEM analysis, a stalked colonial tunicate and two large shells were observed. No such advanced life forms were noted in the treated test chamber (uv-c and solar LEDs), though small crustaceans and shells were observed on both treated and control coupons that may have been deposited after floating in the water column. No hard biofouling such as barnacles were found on either treated or control test coupons, despite barnacles forming on the edges of the test tank. This may indicate an aversion of barnacles to forming on the platinum-coated coupon surfaces, or a combination of conditions within the test chambers that inhibited barnacle growth.

The testing demonstrated some statistical differences in the response variables (biomass and percent cover) between treatment and control chambers, with most of the variation being explained by month rather than treatment type.

In previous experiments (Phase 1 of 3newable's DOE STTR), measurements in a test done in a dockside configuration (Target UV-C dosage was designed for delivery of 40 mJ/cm^2, designated in NSF/ANSI 55 for use in water disinfection), with the UV-C LED operated under the same drive conditions used here had demonstrated that the UV-C LED driven with less than one watt electrical power was able to keep the sample region free of biofouling during a 13-day test period. That was an important first step in demonstrating that our anti-biofouling system could derive sufficient wave power from the wave energy converter that would be responsible for supplying power to the anti-biofouling unit applied to keeping a CTD sensor clean at sea.

The significantly longer test period, with circulating seawater flow used in these experiments, is more representative of a real-world environment and therefore provided a critical step for 3newable to be able to move forward with open ocean testing. Because of the extended period of testing, we designed this system so that images from a camera (as diagrammed in Figure 2) could be uploaded, stored, and observed during the experiment. This design allowed remote monitoring of the temporal evolution of biofouling and provided a useful window with which to observe unexpected phenomena, such as the algae bloom.

7.5 Lessons Learned and Test Plan Deviation

Several modifications were made to the test plan to ensure proper replication across measured response variables and to keep in line with established protocols for biofouling analyses. Biomass weights, staining, and SEM analysis each require separate coupons for analysis and the original test plan did not accommodate an adequate number of replicates for each of the response variables for each sampling interval. In order to preserve triplicate sampling, primary analysis focused on wet weights and staining. This provided compatible, quantitative analyses at each of the three sample points. SEM analysis, which provides a qualitative characterization of biofouling type and coverage, was an additional analysis conducted at the end of the study. Separately, 3newables expressed a desire to forego conductivity testing during this experiment. The conductivity testing would have subjected samples to a potentially destructive process, when proper replication of samples was already a concern. Lacking more than one triplicate group at each timepoint, wet weights and imaging analyses were determined to pose less of a risk to the samples while producing compatible and more valuable results than conductivity testing would have.

Staining and image processing has been emphasized over SEM analysis for use at each sampling interval because it provides numerical values assigned to each coupon based on intensity of biofouling accumulation. This is most informative in distinguishing between variations of light biofouling growth expected to be seen in the uv-c treated samples, but it also quantitatively characterized heavier growth, so the treatment could be numerically compared to control samples.

Last, delays caused by supply chain issues, unexpected required coordination across laboratory teams (e.g. electrical SMEs, ES&H SMEs, and cyber security SMEs), and the reassignment of project investigator due to personnel changes at PNNL have led to minor schedule adjustments. Data points were modified to be at two-, four-, and six-month intervals rather than at one, three, and six months. This allowed for on-schedule analysis with even temporal spacing between data points within the original six-month period of performance for the experiment.

8 Conclusions and Recommendations

There are several conclusions we can draw from the results presented in this report, which 3newable can use to build on for future work.

Adequate power levels under 'real world' conditions: A UV-C LED driven with less than one watt of electrical power was able to prevent 'escalation,' or the evolution from initial formation of biofouling to the eventual establishment of advanced life forms. This is critical real-world information that we were not able to obtain in prior work: either with our first, lab bench level experiments, or during a subsequent 13-day dockside experiment. Results from these experiments done over a time period (months) representative of actual deployments at sea, and using circulating seawater provides 3newable with support that the power level supplied by our wave energy convertor will be sufficient to power a UV-C LED-based anti-biofouling system that can prevent complex life forms from forming on a CTD sensor. With the use of the next generation of UV-C LED light source, we are more confident in the ability of our anti-biofouling system to operate as required on a buoy, powered by the wave energy convertor we are developing.

The need to further investigate fiber-based solutions: Based on the data and discussion presented in 7.4 and 3newable's longer term interest in using fiber technology being developed for efficient delivery of UV-C light to geometries that are challenging to illuminate, 3newable intends to compare our current free-space design with designs that use quartz fiber. We have identified multiple potential sources for UV-C compatible fiber. Protecting fiber used in a design from breaking would be a potential challenge; however, the use of fiber to deliver UV-C light close to the target would allow 3newable to treat more types of sensors and reduce the impact of algae blocking UV-C light before it can reach the area to be treated. Though the algae bloom that occurred during this work was unexpected, it had the effect of underlining the utility of a fiber-based solution in water that might be susceptible to such events. Fibers can deliver UV-C light in confined geometries where, without the use of a fiber, algae could attenuate or completely block UV-C irradiation from reaching critical sensor surfaces. 3newable plans to test designs which incorporate UV-C fibers to address these kinds of issues.

9 REFERENCES

Anderson, M.J., Gorley, R.N. and Clarke, K.R. (2008) PERMANOVA + for PRIMER: Guide to Software and Statistical Methods. PRIMER-E, Plymouth.

F.A.J. Armstrong and G.T. Boalch, Journal of Marine Biology Ass. UK (1961), 41, 591-597, "The Ultra-Violet Absorption of Sea Water"

Larimer C., Winder E., Jeters R., Prowant M., Nettleship I., Addleman R.S., Bonheyo G.T. A method for rapid quantitative assessment of biofilms with biomolecular staining and image analysis. Anal Bioanal Chem. 2016 Jan; 408(3):999-1008. Doi: 10.1007/s00216-015-9195-z. Epub 2015 Dec 7. PMID: 26643074; PMCID: PMC4709385. https://www.ncbi.nlm.nih.gov/pmc/articles/PMC4709385/

Ultraviolet (UV) Water Treatment Systems, NSF/ANSI, 2021, https://blog.ansi.org/nsf-ansi-55-2021-ultraviolet-uv-water-treatment/

10 ACKNOWLEDGEMENTS

PNNL would like to thank research associate Alex Barker for assistance with initial coupon weights and test setup and former PNNL employee Nolann Williams for early experimental coordination. 3newable would like to thank Matt Palanza from the Ocean Observatories Initiative at the Wood's Hole Oceanographic Institute for input on the conclusions section of this report.

Pacific Northwest National Laboratory

902 Battelle Boulevard
P.O. Box 999
Richland, WA 99354

1-888-375-PNNL (7665)

www.pnnl.gov